



# Journal of Applied and Computational Mechanics



Research Paper

## Stress Mode Superposition for a Priori Detection of Highly Stressed Areas: Mode Normalisation and Loading Influence

Carsten Strzalka<sup>1</sup>, Dragan Marinkovic<sup>2</sup>, Manfred W. Zehn<sup>3</sup>

<sup>1</sup> Technical University Berlin, Institute of Mechanics, TU-Berlin, Straße des 17. Juni 135, 10623 Berlin, Germany, Email: carsten.strzalka@tu-berlin.de

<sup>2</sup> Technical University Berlin, Institute of Mechanics, TU-Berlin, Straße des 17. Juni 135, 10623 Berlin, Germany, Email: dragan.marinkovic@tu-berlin.de

<sup>3</sup> Technical University Berlin, Institute of Mechanics, TU-Berlin, Straße des 17. Juni 135, 10623 Berlin, Germany, Email: manfred.zehn@tu-berlin.de

Received February 12 2021; Revised April 12 2021; Accepted for publication April 12 2021.

Corresponding author: C. Strzalka (carsten.strzalka@tu-berlin.de)

© 2021 Published by Shahid Chamran University of Ahvaz

**Abstract.** From the economic and technical point of view, the reduction of development periods and required resources represent a considerable benefit. For the reduction of numerical effort and processed data in numerical stress analysis, the present paper is focused onto the investigation of an efficient method for the *a priori* detection of a structural component's highly stressed areas. Based on the theory of stress mode superposition and the frequency domain solution of the decoupled equations of motion, an analytically consistent approach for *a priori* mode superposition is presented. In this context, the influence of multiaxial loading and mode normalisation is investigated. Validation is performed on a simplified industrial model of a twist-beam rear axle.

**Keywords:** Durability analysis, fatigue hot spot, dynamic stress analysis, high stress prediction, computational efficiency.

### 1. Introduction

In the product development process, numerical methods, as the finite-element-method (FEM), have gained high importance, as comparative studies can be performed in early development stages and cost-intensive experimental investigations can be reduced to a minimum. From an economical point of view, the cost of numerical investigations on the one hand is far lower than that of experiments, on the other hand it is directly connected to the complexity of the investigated models, increasing disproportionately with size, CPU-time and data. Along with high efficiency of modern numerical algorithms [1, 2] as well as widespread availability of computing power and data storage, also the requirements for system size and computational accuracy increase. The tendency towards lightweight structural design resulted in various research directions, such as application of modern composite materials [3, 4], development of modern tools for their modelling and simulation [5, 6], application of smart materials in their design [7, 8], application of methods for structural design optimization [9, 10], etc. Looking at modern lightweight design, mass reduction and extensive exploitation of load bearing capacities lead to higher sensitivity to dynamic stress and failure [11], increasing the requirements of stress accuracy and numerical validation, as the unforeseen failure can cause catastrophic accidents [12]. In that context, especially the stress and durability analysis of dynamically loaded structures still pushes the limits of economically reasonable calculations regarding CPU-time and data. The emerging conflict of high stress accuracy on the one hand and computational speed and efficiency on the other hand, has spawned sophisticated calculation methods in structural dynamics [13]. As direct integration methods can be time consuming and costly, modal approximation methods are well-established in structural dynamics [14]. Based on modal decoupling of the system of equations of motion, a system's response to external excitation can be efficiently calculated and computational cost can be reduced to only a fraction of the direct solution of the full system [15]. Available methods can be categorised in time-domain and frequency-domain approaches, finding application particularly in durability analyses of large structural systems in automotive engineering [16], as well as aerospace, aviation and civil engineering [17]. In well-known mode displacement methods (MDM), independently from time- or frequency-domain, the system's physical displacement-response is approximated by linear superposition of generalised coordinates and corresponding natural modes [18]. The resulting stress fields are post-processed from the superimposed field of displacements, in which more than 99 % of CPU-time may be used for data recovery for large models and long loading events [19]. As the type of mode-normalisation has generally no influence on the results of physical stress analyses, the effect of mode-scaling is typically investigated in the field of experimental modal analysis and system identification [20-23]. For higher numerical efficiency, modal strain and modal stress methods have gained high importance especially in durability and numerical fatigue analyses. The basic concept of modal strain roots in experimental modal analysis from strain measurements and is well-described in [24]. Yet, modal stress superposition techniques have been pertained in numerous applications in time-domain [25, 26], as well as frequency-domain [27-29] for all types of technically relevant loading. The general procedure of stress mode superposition has been extended to more specific modal fields, as modal stress intensity factors [30] and finds application in flexible multibody dynamics [31], submodeling approaches [32] and extended finite element methods [33] to account for local plasticity phenomena.



As typically high stress concentration in large systems is locally limited to only small areas of the global model, the *a priori* identification of these highly stressed regions is of great advantage for the reduction of numerical effort of any present or subsequent analysis steps. In automotive industry, the fraction of a model being of considerable durability interest is around 1% [34]. Especially in numerical fatigue analysis, which is an additional post-process to the dynamic stress analysis, filtering of so-called hot spot areas plays an important role, as the complex analysis of stress data of long loading events increases computational effort [35]. Most existing algorithms for detecting high stress in structural components can be summarized as *posteriori* methods, as they rely on the analysis of present stress history data. Huang et al. [19], for instance, perform an element pre-scan for elements exceeding a threshold value of von Mises stress in short peak loading events on vehicle body structures. Full stress history analysis and fatigue-life evaluation are subsequently limited to the top 100 elements, resulting in a method for identifying highly stressed elements [36]. Besides the application of modal methods for the calculation of structural stress responses, eigenvectors and their derivatives find wide application in many fields of engineering research [37], as model updating [38], structural health monitoring [39] and damage detection [40], optimization [41] and model order reduction.

Apart from the established methods, the system's information inherent in the eigenvectors and especially in the resulting stress mode shapes, can be applied for the development of powerful methods for *a priori* high stress detection. Veltri [42] describes a method for the *a priori* prediction of stress concentration based on component-mode-synthesis (CMS) methods for the durability analysis of an all-terrain vehicle frame subjected to road-load time histories. Information about highly stressed elements is gained from selected fixed interface normal modes, while the influence of external loading is captured by a set of static modes. For numerical fatigue analysis of plate-type structures subjected to random base excitation, Zhou et al. [43] propose a procedure for locating highly stressed elements from modal stress analyses. A Subsequent durability analysis is carried out in the frequency domain and, for reduction of computational effort, is limited to the detected hot spots. For a notched elbow structure under base-excitation, Zhou et al. [44, 45] later interpreted the contributions of dominant modes from mass modal participation factors and perform random vibration fatigue analyses on the so determined hot spots.

In this paper, an *a priori* stress mode superposition approach is investigated for force excited systems. By means of appropriate approximation and prediction of maximum modal contributions, a weighting coefficient for *a priori* superposition of modal von Mises stress fields is developed from the frequency domain solution of the decoupled equations of motion in modal space. Loading influence is captured by modal load considerations, as recent investigation [46] explains in more detail. In addition, the general influence of mode normalisation is investigated on a simply supported cantilever beam structure. The developed approach is then validated on the simplified industrial model of a twist-beam rear axle with multiaxial loading on variable loading positions. The innovation of this approach is based on the fact that the required information is limited to the system's normal modes and basic loading information in terms of the areas of load application and directions. As a structural system's fundamental dynamic properties, the elastic normal modes are determined in early product development stages. The presented methodology extends the existing modal mass participation considerations (e.g. [44, 45]) to force excited systems. In this manner, detailed engineering assessment is eliminated, thus making the approach significantly more efficient and therewith readily applicable to automated computations and optimization algorithms. The paper is structured as follows: In section 2, the basic equations of mode superposition are summarized and the theory of stress mode superposition in the frequency domain is given in section 3. In section 4, a weighting coefficient for *a priori* application is derived to approximate the dominant modes' maximum contributions to the system's response whereas special attention is paid to mode normalisation. For validation, the proposed approach is applied to the rear axle example in section 5, followed by a summary and conclusion in section 6.

## 2. Mode Superposition

A structure discretised by finite elements is described by a system of differential equations (1), with the system's mass matrix  $\mathbf{M}$ , damping matrix  $\mathbf{C}$  and stiffness matrix  $\mathbf{K}$ , the vectors of nodal accelerations  $\ddot{\mathbf{u}}(t)$ , nodal velocities  $\dot{\mathbf{u}}(t)$ , nodal displacements  $\mathbf{u}(t)$  and the vector of external excitations  $\mathbf{F}(t)$ .

$$\mathbf{M}\ddot{\mathbf{u}}(t) + \mathbf{C}\dot{\mathbf{u}}(t) + \mathbf{K}\mathbf{u}(t) = \mathbf{F}(t) \quad (1)$$

In order to approximate the structure's dynamic displacement field, the system can be transformed to modal space. In this manner the displacement field is given by linear superposition of the system's eigenvectors,  $\boldsymbol{\varphi}_i$ , and generalised coordinates,  $q_i$ . Solving the eigenvalue problem of the undamped system (2), the eigenvalues,  $\omega_{0,i}^2$ , and the corresponding eigenvectors,  $\boldsymbol{\varphi}_i$ , are determined:

$$(\mathbf{K} - \omega_{0,i}^2 \mathbf{M})\boldsymbol{\varphi}_i = 0 \quad (2)$$

With the eigenvectors arranged as columns of the modal matrix  $\mathbf{X}$ , the transformation of the system to modal space is performed:

$$\mathbf{u}(t) = \sum_i^r \boldsymbol{\varphi}_i q_i(t) = \mathbf{X}\mathbf{q}(t) \quad (3)$$

From the modes' orthogonality properties, assuming modal damping, the equations of motion decouple. Transformation of the system matrices yields:

$$\mathbf{X}^T \mathbf{M} \mathbf{X} = \text{diag}(m_i) \quad ; \quad \mathbf{X}^T \mathbf{C} \mathbf{X} = \text{diag}(c_i) \quad ; \quad \mathbf{X}^T \mathbf{K} \mathbf{X} = \text{diag}(k_i) \quad (4)$$

$$\begin{bmatrix} m_1 & \dots & 0 \\ \vdots & \ddots & \vdots \\ 0 & \dots & m_r \end{bmatrix} \begin{bmatrix} \ddot{q}_1(t) \\ \vdots \\ \ddot{q}_r(t) \end{bmatrix} + \begin{bmatrix} c_1 & \dots & 0 \\ \vdots & \ddots & \vdots \\ 0 & \dots & c_r \end{bmatrix} \begin{bmatrix} \dot{q}_1(t) \\ \vdots \\ \dot{q}_r(t) \end{bmatrix} + \begin{bmatrix} k_1 & \dots & 0 \\ \vdots & \ddots & \vdots \\ 0 & \dots & k_r \end{bmatrix} \begin{bmatrix} q_1(t) \\ \vdots \\ q_r(t) \end{bmatrix} = \mathbf{X}^T \mathbf{F}(t) \quad (5)$$

From each row of eq. (5), the frequency domain solution for a harmonic excitation  $\mathbf{F}(t) = \hat{\mathbf{F}}e^{i\Omega t}$  can be formulated and the modal coordinates  $q_i$ , modal velocities  $\dot{q}_i$  and modal accelerations  $\ddot{q}_i$  can be evaluated for the forced vibration problem.

$$(-\Omega^2 + 2\mathfrak{D}_i \omega_{0,i} i\Omega + \omega_{0,i}^2) \hat{q}_i e^{i\Omega t} = \frac{\hat{f}_i}{m_i} e^{i\Omega t} \quad (6)$$



With the modal load  $\hat{f}_i$  for each mode,

$$\hat{f}_i = \boldsymbol{\varphi}_i^T \hat{\mathbf{F}} \quad (7)$$

the system's frequency dependent modal response amplitude  $\hat{q}_i$  for each modal coordinate is given by:

$$\hat{q}_i(\Omega) = \frac{1}{(-\Omega^2 + 2\vartheta_i \omega_{0,i} i\Omega + \omega_{0,i}^2)} \omega_{0,i}^2 \frac{\hat{f}_i}{k_i} \quad (8)$$

Furthermore, with the frequency ratio  $\eta_i = \Omega / \omega_{0,i}$ , the complex frequency response function  $H^q(\eta)$  in generalised coordinates is defined and the steady state response can be written as

$$\hat{q}_i(\eta) = H^q(\eta) \hat{f}_i \quad (9)$$

Transforming back to physical coordinates by means of the following equation:

$$\hat{\mathbf{u}}(\eta) = \mathbf{X} \hat{\mathbf{q}}(\eta) \quad (10)$$

the system's complex frequency response function,  $H(\eta)$ , in physical coordinates can be evaluated for the steady state solution for the forced harmonic excitation as given below:

$$\mathbf{H}(\eta) = \sum_{i=1}^r \boldsymbol{\varphi}_i \boldsymbol{\varphi}_i^T \frac{((1 - \eta_i^2) - i2\vartheta_i \eta_i)}{k_i ((1 - \eta_i^2)^2 + 4\vartheta_i^2 \eta_i^2)} \quad (11)$$

Finally, from the corresponding displacement field given in eq. (12), the resulting time-dependent strain and stress for each excitation frequency  $\Omega$  can easily be evaluated.

$$\mathbf{u}(t) = \sum_{i=1}^r \boldsymbol{\varphi}_i \boldsymbol{\varphi}_i^T \frac{((1 - \eta_i^2) - i2\vartheta_i \eta_i)}{k_i ((1 - \eta_i^2)^2 + 4\vartheta_i^2 \eta_i^2)} \hat{\mathbf{F}} e^{i\Omega t} \quad (12)$$

### 3. Modal Stress Approach

For the reduction of numerical effort needed for stress recovery in linear systems, a modal stress approach, also called matrix method as the stress modes can be arranged to a modal stress matrix, has been well-established over the last decades [19]. Equivalent to the displacement modes, also the so-called strain modes  $\boldsymbol{\Psi}_i$  are capable of describing the dynamic properties of vibrating structures. Application of the differential operator  $\mathbf{D}$  to the displacement modes yields the strain modes for the FE-discretised structure:

$$\boldsymbol{\Psi}_i = \mathbf{D} \boldsymbol{\varphi}_i \quad (13)$$

By linear superposition of the contributions of modal strain fields, the structure's dynamic strain response  $\boldsymbol{\varepsilon}$  and, for a linear-elastic and homogeneous material, the corresponding stress response  $\boldsymbol{\sigma}$  is determined by using the Hooke's matrix  $\mathbf{H}$  [24]:

$$\boldsymbol{\varepsilon} = \sum_{i=1}^r q_i \boldsymbol{\Psi}_i \quad ; \quad \boldsymbol{\sigma} = \sum_{i=1}^r q_i \mathbf{H} \boldsymbol{\Psi}_i \quad (14)$$

From the modal stress approach, we find the complex stress transfer function  $\mathbf{H}^\sigma(\eta)$  and corresponding steady state solution for the physical stress field  $\boldsymbol{\sigma}(t)$ :

$$\mathbf{H}^\sigma(\eta) = \sum_{i=1}^r \mathbf{H} \boldsymbol{\Psi}_i \boldsymbol{\varphi}_i^T \frac{((1 - \eta_i^2) - i2\vartheta_i \eta_i)}{k_i ((1 - \eta_i^2)^2 + 4\vartheta_i^2 \eta_i^2)} \quad (15)$$

$$\boldsymbol{\sigma}(t) = \sum_{i=1}^r \mathbf{H} \boldsymbol{\Psi}_i \boldsymbol{\varphi}_i^T \frac{((1 - \eta_i^2) - i2\vartheta_i \eta_i)}{k_i ((1 - \eta_i^2)^2 + 4\vartheta_i^2 \eta_i^2)} \hat{\mathbf{F}} e^{i\Omega t} \quad (16)$$

Additionally, with the tensorial strain- and stress-mode-shapes given in eq. (14), one can apply the well-known strength theories to determine stress measure mode-shapes such as principal stress modes, equivalent von Mises stress modes or strain energy modes, which can also be used in the mode superposition approach.

### 4. A Priori Mode Superposition

In many applications of numerical stress and durability analysis, the knowledge of highly stressed regions, i.e. sets of finite elements, is of great advantage and therefore of high interest to structural engineers. In the following, an approach is developed for a *priori* detection of these highly stressed elements, based on modal stress superposition techniques. As a mechanical component's dynamic response and the corresponding stress are always a function of its excitation, for the development of an *a priori* mode superposition approach, the influence of loading position and loading direction plays a crucial role. Solution of the system's eigenvalue problem yields scalable eigenvectors and therefore special attention needs to be paid to mode normalisation and the influence on the resulting modal stress fields. Starting from the system's complex transfer function in modal coordinates given in eq. (8), we find the real valued amplification function  $V(\eta_i)$  for each mode:



$$V(\eta_i) = \frac{1}{k_i \sqrt{(1 - \eta_i^2)^2 + 4\eta_i^2}} \tag{17}$$

The frequency ratio for the maximum amplification at resonance  $\eta_{res,i}$  is found from the derivation of the amplification function of the underdamped system, i.e. for  $\eta \leq \sqrt{2} / 2$ :

$$\eta_{res,i} = \sqrt{1 - \eta_i^2} \quad ; \quad \Omega_{res,i} = \omega_{0,i} \sqrt{1 - \eta_i^2} \tag{18}$$

From equations (8) and (18), the maximum modal contributions at resonance  $\hat{q}_{i,max}$  can be written as

$$\hat{q}_{i,max} = \frac{\hat{f}_i}{k_i 2\eta_i \sqrt{1 - \eta_i^2}} \tag{19}$$

The maximum stress response in frequency domain can then be approximated as

$$\sigma_{max}(\Omega) = \sum_{i=1}^r \mathbf{H}\Psi_i \frac{\hat{f}_i}{k_i 2\eta_i \sqrt{1 - \eta_i^2}} \tag{20}$$

### 4.1 Loading Influence

Expanding the assumptions of the previous section, separation of the system's excitation to one vector of loading functions  $\mathbf{p}$ , with each entry  $p_j$  accounting for time-dependency in the  $j^{th}$  degree of freedom, and one spacial force-direction vector  $\mathbf{f}$ , yields a means for a priori application of the modal stress superposition, where the influence of loading position and direction is captured by the dot-product of an eigenvector and force-direction vector, also accounting for multiaxial loading configurations.

$$\hat{f}_i = \boldsymbol{\varphi}_i^T \mathbf{f} \mathbf{p} \tag{21}$$

We hereby find a weighting coefficient  $\Gamma_i$  as an approximation that accounts for the modal contributions to the overall vibration and, as discussed in the following section, also for mode normalisation for an a priori superposition of modal fields. The assumption that all modal maxima are in-phase, results in an upper bound for maximum dynamic stress. Assuming the frequency content of  $\mathbf{p}$  induces all mode-shapes to respond at resonance, the superposition of all amplitude maxima resembles the assumptions of the well-established response spectrum analysis [47].

$$\Gamma_i = \frac{\boldsymbol{\varphi}_i^T \mathbf{f}}{k_i 2\eta_i \sqrt{1 - \eta_i^2}} \quad ; \quad \sigma_{max} = \sum_{i=1}^r \mathbf{H}\Psi_i \Gamma_i \tag{22}$$

### 4.2 Mode Normalisation

Eigenvectors calculated by commercial modal analysis tools are scalable and, commonly, either unit displacement or unit mass normalised. A physical interpretation of the effect of scaling of eigenvectors to unit length or unit modal mass, respectively, is given in [48]. In this paper, modal stiffness normalisation is proposed.

The simple example of a beam structure shown in Fig. 1 illustrates the effects of this approach on resulting modal fields. The cantilever beam (length of 1 m, square cross-section of 10 x 10 mm<sup>2</sup>, material properties of steel, as depicted in table 1) is additionally simply supported at its right end and discretised with 15 linear beam elements, type B31 in commercial FE-software ABAQUS. In the following, the von Mises modal stress is considered for stress mode superposition. As an equivalent stress measure, it is independent from the sign of any modal scaling factor, making it well applicable for a priori superposition on the one hand, and, on the other hand, it is a well-established stress measure for evaluation of multiaxial stress states.

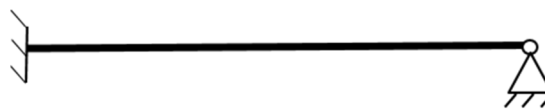


Fig. 1. Cantilever beam example

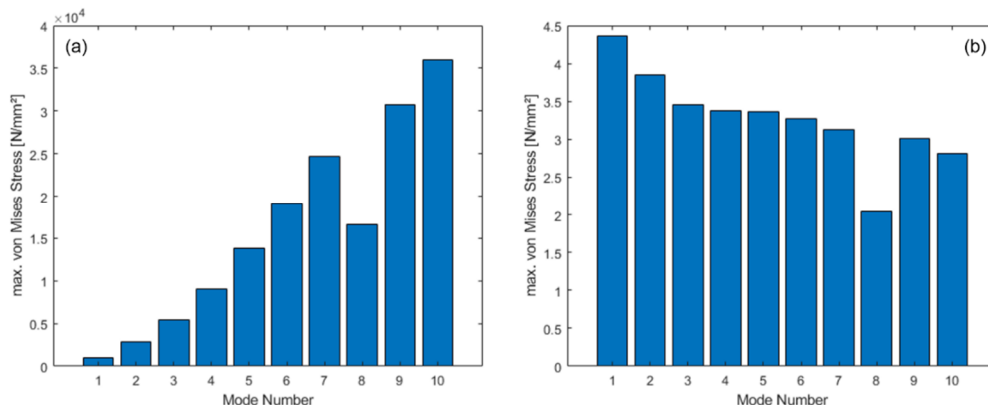


Fig. 2. Maximum von Mises stress for each mode: (a) unit mass normalisation, (b) unit stiffness normalisation



With the unit mass mode normalisation, the resulting modal fields show a significant change (mainly increase) in the maximum local modal stress going from the first to higher modes. This is represented in Fig. 2a for the first 10 von Mises stress modes. One should keep in mind that the lower modes are often dominant in a dynamic structural response.

As local stress maxima of higher modes would overlay or mask the dominant global maxima, a general stress mode superposition using unit mass normalisation is not applicable for *a priori* superposition. In the proposed approach, unit modal stiffness normalisation is proposed. Hence, an eigenvector  $\varphi_i$  is determined so that the modal stiffness  $k_i$  equals 1:

$$\varphi_i^T \mathbf{K} \varphi_i = k_i \equiv 1 \tag{23}$$

Finding a constant factor  $a_i$  to perform the normalisation,

$$\bar{\varphi}_i = a_i \varphi_i \quad \rightarrow \quad \bar{\varphi}_i^T \mathbf{K} \bar{\varphi}_i = 1 \tag{24}$$

the unit stiffness-normalised eigenvector  $\bar{\varphi}_i$  is defined in eq. (25), while the same transformation is also valid for the corresponding strain  $\bar{\Psi}_i$  and stress modes, respectively.

$$\bar{\varphi}_i = \frac{1}{\sqrt{k_i}} \varphi_i \quad ; \quad \bar{\Psi}_i = \frac{1}{\sqrt{k_i}} \Psi_i \tag{25}$$

Equation (23) reveals a direct relation between the modal stiffness and the strain energy content of a mode. Hence, unit modal stiffness normalisation can also be interpreted as modal strain energy normalisation. The distribution of the resulting maximum element stress over the 10 mode shapes depicted in Fig. 2b is significantly more uniform compared to the result from the unit mass normalisation. Now, the maximum frequency domain solution for stress can be transformed to the physical coordinates (eq. (20)), which is independent from the mode normalisation approach. By means of equations (14) and (21), the maximum stress response can be rewritten and decomposed into a term solely dependent on the system's individual properties (the Hooke's matrix  $\mathbf{H}$ , modal stiffness  $k_i$ , damping  $\vartheta_i$  and the eigenvectors  $\varphi_i$ ) and a term related to the spatial distribution of the loading  $\mathbf{f}$ . As the maximum response is considered at each modal resonance:

$$\sigma_{\max} = \sum_{i=1}^r \frac{1}{k_i} \frac{\mathbf{H} \mathbf{D} \varphi_i \varphi_i^T \mathbf{f}}{2 \vartheta_i \sqrt{1 - \vartheta_i^2}} \tag{26}$$

the frequency dependency is eliminated.

As the physical stress field is independent from any mode normalisation, division by modal stiffness  $k_i$  in equations (22) and (26), can be interpreted as re-normalisation of an eigenvector with respect to the modal stiffness. Combining equations (25) and (26) in eq. (27), we find proof for the derivation of an analytically and physically consistent weighting coefficient  $\Gamma_i$  for stress mode superposition in eq. (22).

$$\sum_i \frac{\mathbf{H} \bar{\Psi}_i \bar{\varphi}_i^T \mathbf{f}}{\sqrt{k_i} \sqrt{k_i} 2 \vartheta_i \sqrt{1 - \vartheta_i^2}} = \sum_i \frac{1}{k_i} \frac{\mathbf{H} \mathbf{D} \varphi_i \varphi_i^T \mathbf{f}}{2 \vartheta_i \sqrt{1 - \vartheta_i^2}} = \sum_i \mathbf{H} \Psi_i \Gamma_i \tag{27}$$

### 5. Industrial Example

For validation of the developed approach, a simplified beam model of the twist-beam rear axle depicted in Fig. 3a, is investigated. For general investigations, the complex geometry of the real axle is defeatured and simplified to enable modeling with beam elements and excluding the effects of local details. To meet the global dynamic properties of the real model in the lower eigenfrequencies with similar global mode shapes, the properties of the simplified model have been adapted.

The simplified model is discretised with an average element length of 1 mm (1876 linear beam elements of type B31, circular cross-section of 40 mm in diameter), material properties are depicted in table 1. Boundary conditions at the sleeve positions for axle bushings are fixed, with free rotation around the local x-axes, at the areas of stub-axle assembly, one side is free, and one side is encastered, as depicted in Fig. 3b.

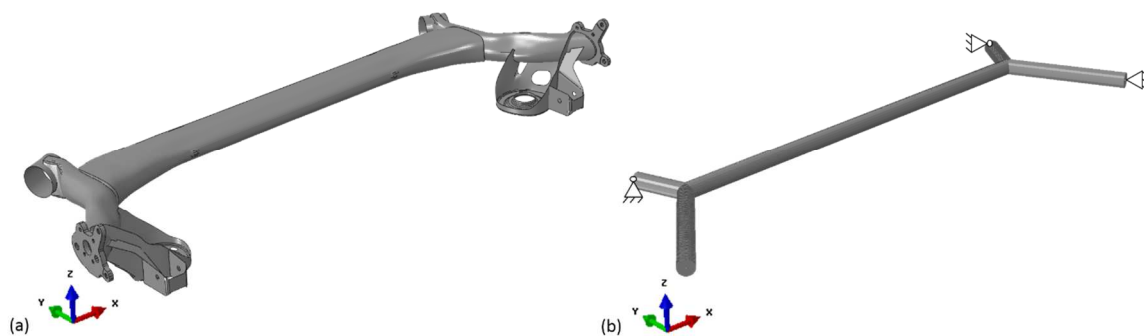


Fig. 3. (a) Industrial model and (b) simplified beam model



Table 1. Material Properties

| Young's Modulus [MPa] | Density [t/mm <sup>3</sup> ] | Poisson ratio [1] |
|-----------------------|------------------------------|-------------------|
| 220 000               | 7.85                         | 0.3               |

The influence of the loading position of a unidirectional loading on the resulting stress field has been investigated in [46]. This investigation is focused on the loading influence in more complex multiaxial loading configurations. For this purpose, the system's steady state response is analysed for 4 multiaxial loading configurations depicted in Fig. 4, whereby modal decoupling is used with the first 10 modes in a frequency range of up to 1000 Hz with a frequency step of  $\Delta f = 1$  Hz and critical damping of  $\eta = 0.2$ . In Fig. 4, one can interpret the first load-case (LC-1) as vertical and horizontal forces, resulting from road-load excitation, whereas the other load-cases are more of academic interest, as they do not represent loading-events from the structure's actual field of application.

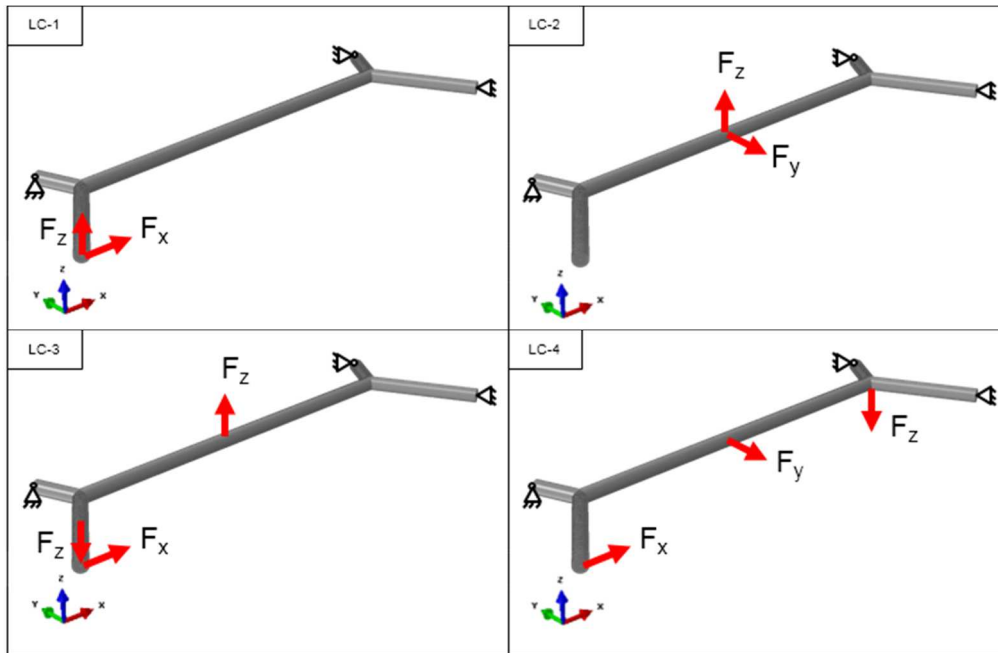


Fig. 4. Investigated Multiaxial load-cases

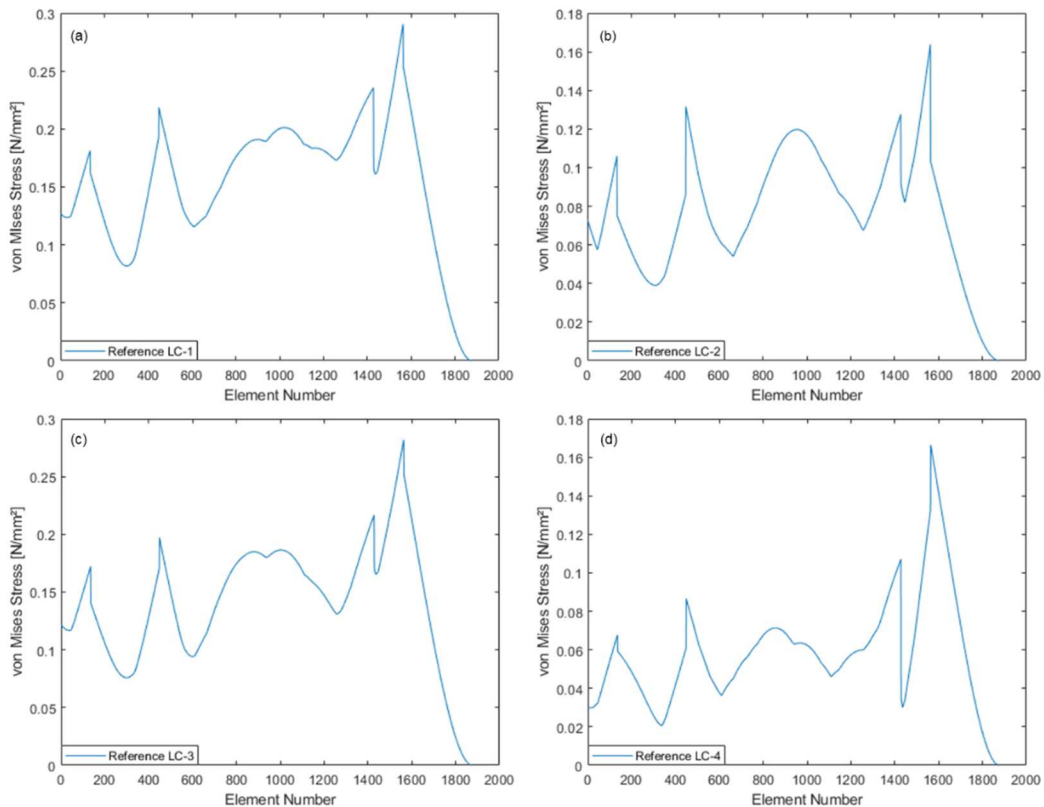


Fig. 5. Reference solution: von Mises stress for all elements: a) load-case 1; b) load-case 2; c) load-case 3; d) load-case 4



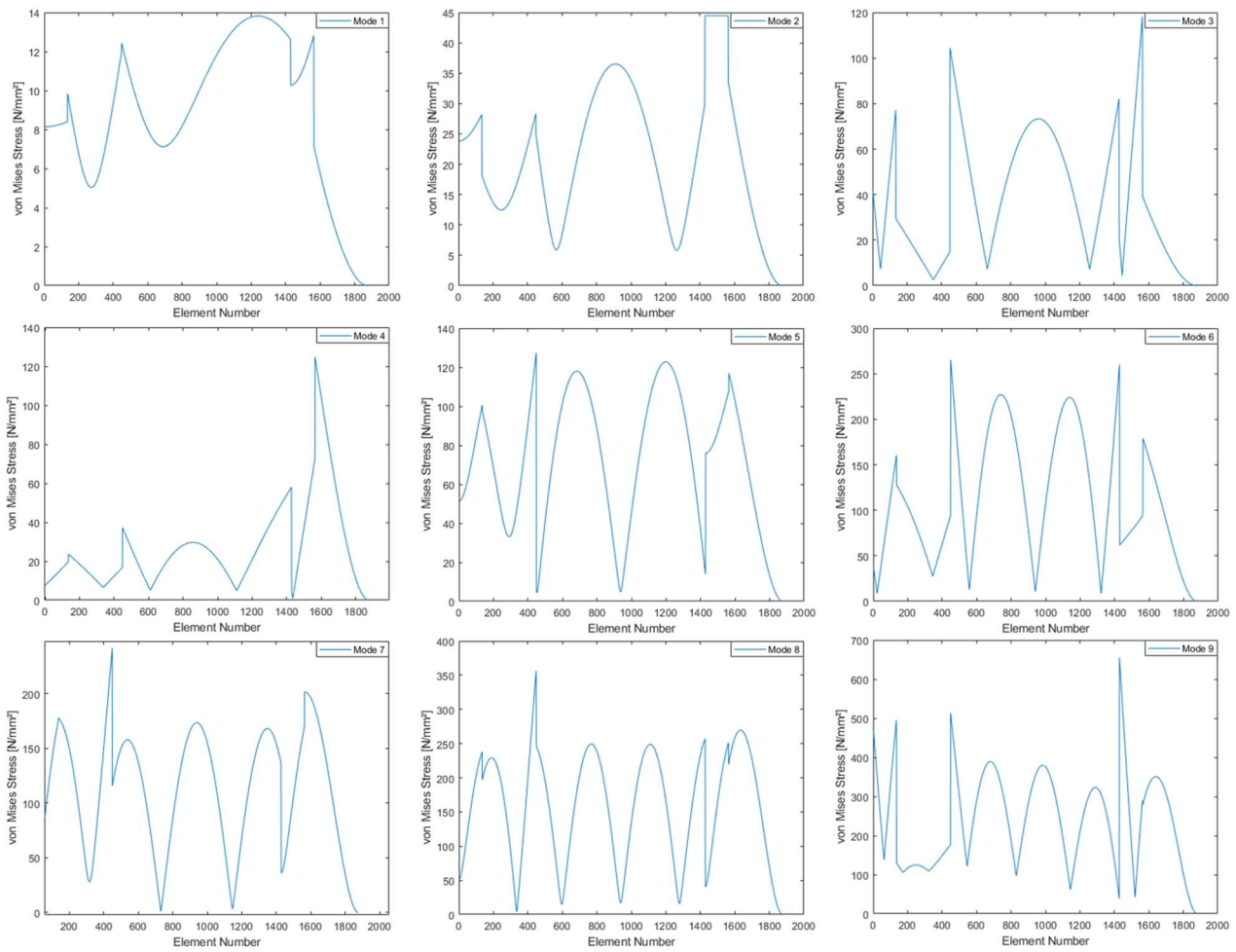


Fig. 6. First 9 von Mises stress modes

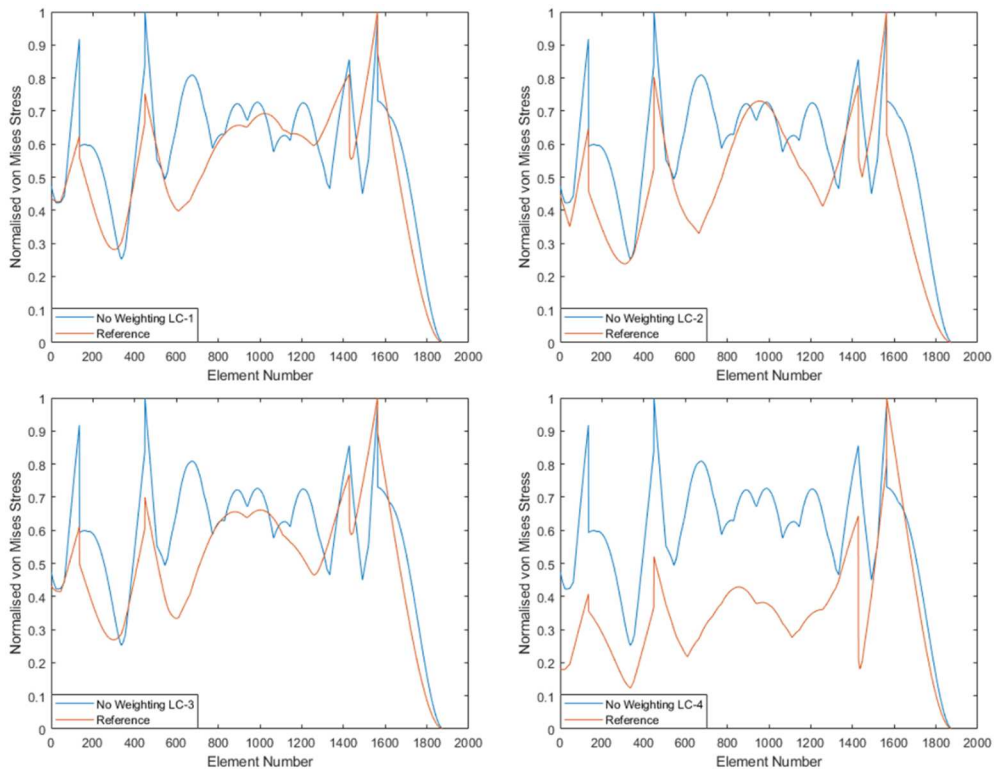


Fig. 7. Mode superposition with no weighting of considered modes (normalised results)



As a reference solution, the von Mises stress is evaluated by superimposing the maxima of the first 10 modal coordinates with each corresponding stress mode, as derived in section 3. The resulting stress over all elements is shown for all load-cases in Fig. 5.

For interpretation of the resulting superimposed stress fields, the first 9 von Mises stress modes, resulting from mass-normalised eigenvectors, are depicted in Fig. 6. While 10 modes have been considered for mode superposition in the example, mode 10 is not shown for layout reasons.

Figure 6 clearly reveals that the local stress magnitude increases for higher modes, which was already derived in section 4.2 for the unit mass normalised eigenvectors. Direct superposition of these stress modes leads to high deviations with respect to the reference solution. As the resulting stress ranges differ in orders of magnitude, comparison is only possible with the normalised results, Fig. 7. Direct superposition does not account for loading information and, consequently, the results by direct superposition are identical for all load-cases.

In the next step, the influence of the modal load is investigated and for this purpose the superposition is performed with modal load from eq. (7) as weighting coefficient. As seen in Fig. 8, the weighted superposition, by using the modal load coefficients only, yields no improvement of the results and is therefore not applicable for *a priori* methods.

The modal contributions of the reference solution for each load-case are given in Fig. 9. The figure makes it obvious that the higher stress modes are less dominant in the excitation. However, with the unit mass normalisation applied, the resulting stress magnitudes are much higher for higher modes. As a consequence, the influence of lower modes, which are in fact dominant in the structural response, is masked by the artificially increased influence of the higher modes in the resulting superimposed stress fields. The effect becomes even more pronounced with a wider frequency range considered.

Application of the proposed weighting coefficient improves the results, as derived in section 4. Comparison of the reference solution with the results of the proposed *a priori* superposition shows the exact match, as seen in Fig. 10. The proposed weighting coefficients have three important features:

- the modal loads are used in determination of the modal contributions,
- the maximum modal frequency-domain responses are also accounted for,
- and the modal strain energy content is considered for mode normalisation.

From the results of *a priori* stress mode superposition, high stress regions can be readily detected using a threshold criterion, as proposed in [36]. As the procedure is based on scalable modal fields, the assessment should be performed qualitatively. For instance, depending on the field of application and severity of unexpected failures, elements that exceed a stress-limit of 70 % of the maximum occurring stress can be considered as elements of interest. As depicted in Fig. 11, plausible results on high stress regions for the investigated example can be achieved (high-stress elements marked in red), with the clear indication of the influence of different loading configurations.

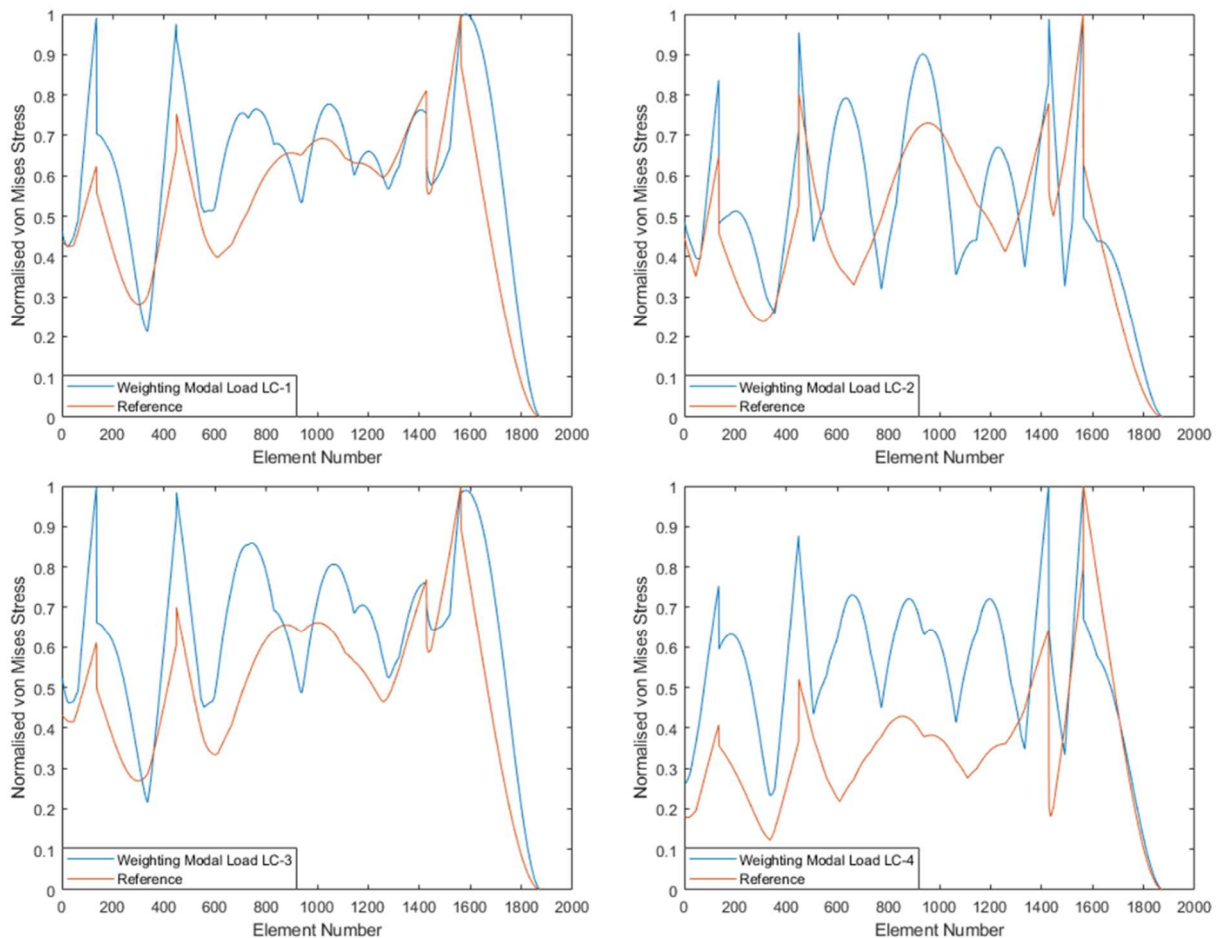


Fig. 8. Mode superposition, weighting with modal load coefficient (normalised results)



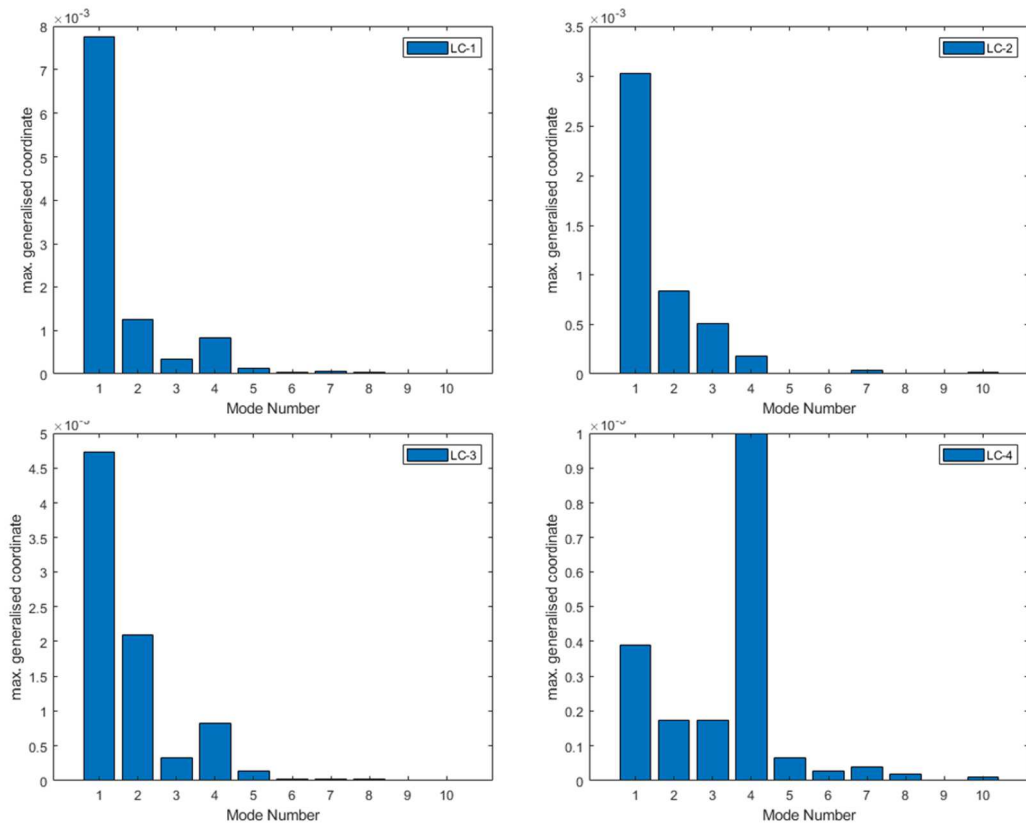


Fig. 9. Maximum modal contributions from reference solutions for all load-cases

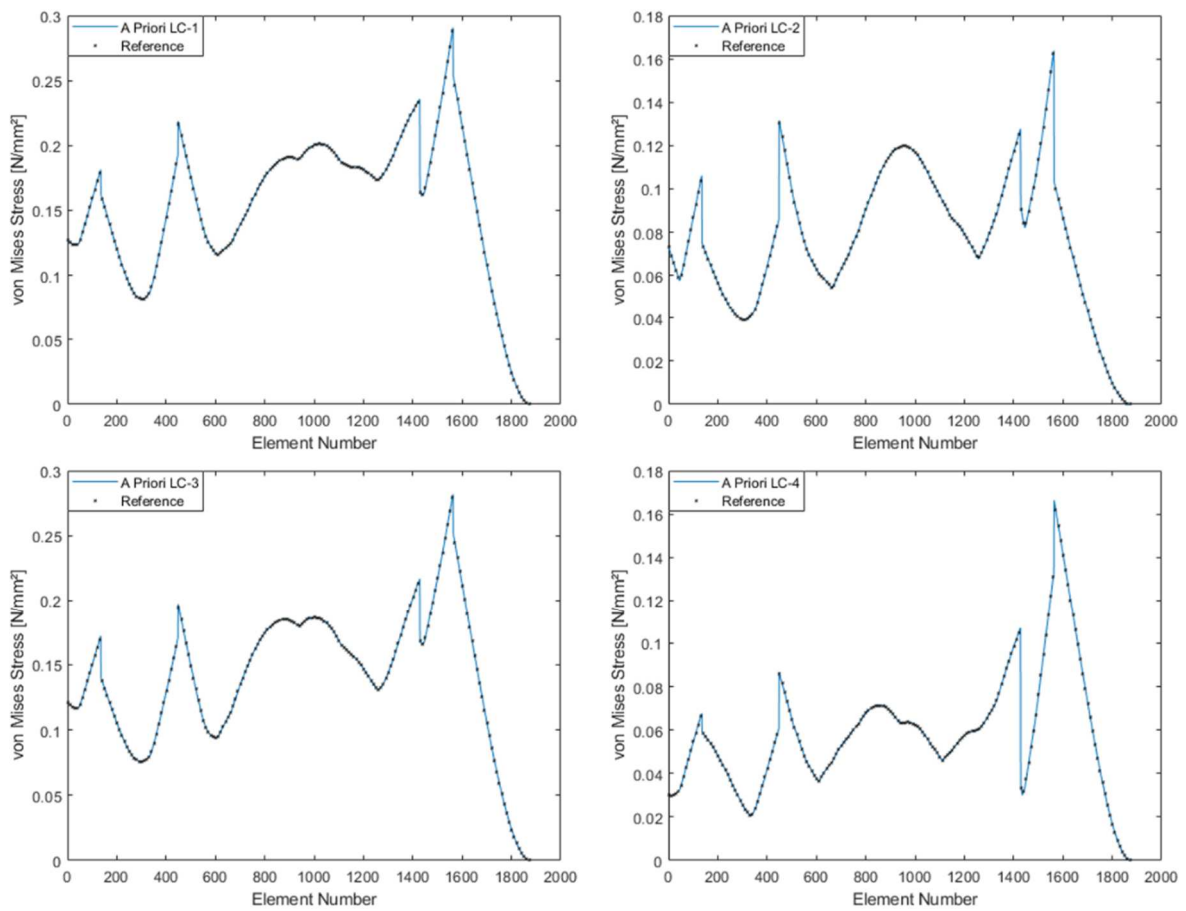


Fig. 10. Comparison of proposed a priori superposition and reference solutions (exact match)



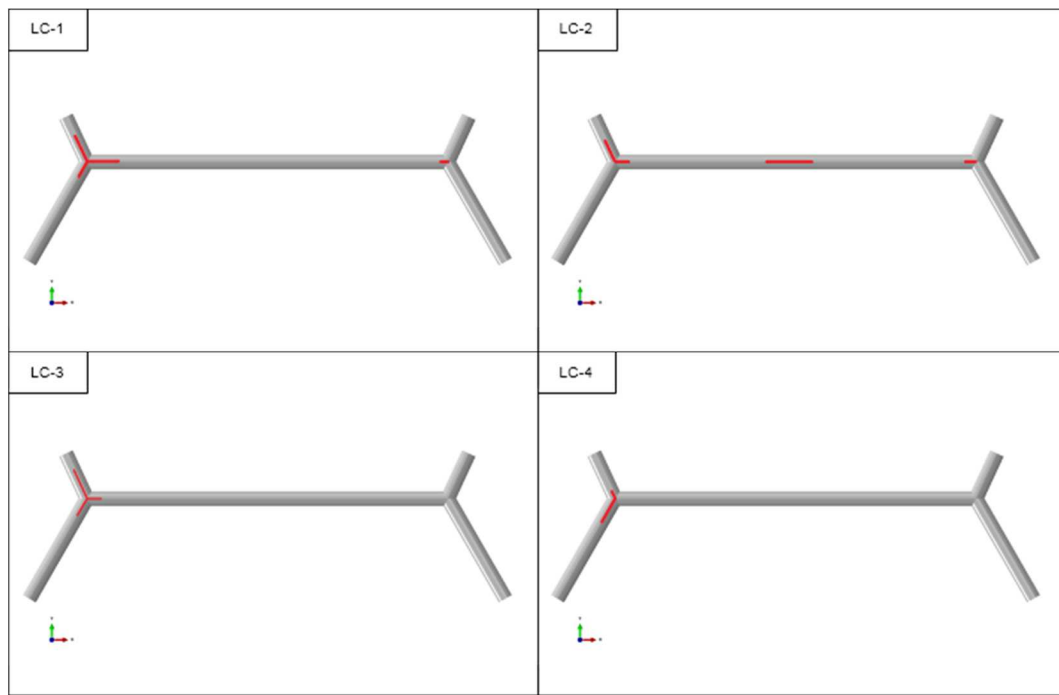


Fig. 11. Results of high stress detection for threshold 70 % of maximum stress

## 6. Summary and Conclusion

The paper elaborates *a priori* detection of highly stressed structural regions by means of a modal stress superposition approach. The objective was to develop and validate a methodology for this purpose, which is applicable to force excited structural components prior to cost-intensive calculations in order to reduce the computational effort significantly in subsequent analysis steps. The investigation was focused on the influence of mode normalisation and loading configurations on the results of *a priori* stress mode superposition. The simply supported beam structure revealed the aspects of mode normalisation. A relation between the modal stiffness and modal strain energy content was demonstrated and the mode normalisation with respect to the system's stiffness matrix was proposed to overcome the effect of masking of dominant modes in an *a priori* mode superposition procedure. For determination of maximum contributions of dominant modes, the frequency domain solution of the decoupled equations of motion was employed together with the modal load considerations, thus leading to an analytically consistent weighting coefficient for *a priori* superposition. For validation, a simplified industrial model has been investigated under complex multiaxial loading conditions at variable positions. Reference solutions were obtained by superposition of the maxima of the generalised coordinates from modally decoupled steady state analyses, resembling the assumptions of response spectrum analyses. From superposition of modal von Mises stress fields, the results of reference solution and the proposed approach show exact match. The stress fields approximated in this manner deliver valuable information about highly stressed elements with a low computational cost. With that knowledge, sophisticated subsequent analysis steps can be limited to only fractions of the global model, e.g. submodeling, substructuring or crack propagation analyses, providing high potential for data reduction and increasing efficiency. In contrast to existing approaches, by introduction of the proposed weighting coefficient, *a priori* applicability as well as reliability and performance can be increased to a great extent. A great advantage of the proposed approach is seen in the fact that it is applicable in relatively early stages of product development.

## Author Contributions

C. Strzalka developed the basic concept and mathematical modeling, performed numerical investigations and examined the theory validation; D. Marinkovic and M. Zehn contributed to the development of the methodology; The manuscript was written through the contribution of C. Strzalka and D. Marinkovic; M. Zehn supervised the project; All authors discussed the results, reviewed, and approved the final version of the manuscript.

## Conflict of Interest

The authors declared no potential conflicts of interest with respect to the research, authorship, and publication of this article.

## Funding

The authors received no financial support for the research, authorship, and publication of this article.

## Nomenclature

|              |                           |                    |                             |
|--------------|---------------------------|--------------------|-----------------------------|
| $a_i$        | Normalising factor [-]    | $\hat{\mathbf{q}}$ | Modal amplitude vector [m]  |
| $\mathbf{C}$ | Damping matrix [kg/s]     | $\hat{q}_{i,\max}$ | Maximum modal amplitude [m] |
| $c_i$        | Modal damping [kg/s]      | $\mathbf{u}$       | Displacement [m]            |
| $\mathbf{D}$ | Differential operator [-] | $\dot{\mathbf{u}}$ | Velocity [m/s]              |



|                           |  |                     |   |
|---------------------------|--|---------------------|---|
| $\mathbf{F}(t)$           | Forcing function [N]                           | $\ddot{\mathbf{u}}$ | Acceleration [m/s <sup>2</sup> ]            |
| $\hat{f}_i$               | Modal load [N]                                 | $\hat{\mathbf{u}}$  | Displacement amplitude [m]                  |
| $\hat{\mathbf{f}}$        | Force amplitude vector [N]                     | $V(\eta_i)$         | Amplification function [-]                  |
| $\mathbf{f}$              | Force-direction vector [-]                     | $\mathbf{X}$        | Modal matrix [-]                            |
| $\mathbf{H}$              | Hooke's matrix [N/m <sup>2</sup> ]             | $\Gamma_i$          | Weighting coefficient [-]                   |
| $\mathbf{H}^\sigma(\eta)$ | Stress transfer function [1/m <sup>2</sup> ]   | $\epsilon$          | Strain tensor [-]                           |
| $\mathbf{H}(\eta)$        | Displacement transfer function [m/N]           | $\eta_i$            | Frequency ratio [-]                         |
| $H^q(\eta)$               | Modal transfer function [m/N]                  | $\eta_{res}$        | Resonance frequency ratio [-]               |
| $\mathbf{K}$              | Stiffness matrix [N/m]                         | $\sigma$            | Stress tensor [N/m <sup>2</sup> ]           |
| $k_i$                     | Modal stiffness [N/m]                          | $\sigma_{max}$      | Maximum stress tensor [N/m <sup>2</sup> ]   |
| $\mathbf{M}$              | Mass matrix [kg]                               | $\varphi_i$         | Eigenvector [-]                             |
| $m_i$                     | Modal mass [kg]                                | $\bar{\varphi}_i$   | Normalised eigenvector [1 / $\sqrt{N/m}$ ]] |
| $\mathbf{p}$              | Vector of time-dependent forcing functions [N] | $\Psi_i$            | Strain mode [-]                             |
| $\mathbf{q}$              | Vector of modal coordinates [m]                | $\bar{\Psi}_i$      | Normalised strain mode [1 / $\sqrt{N/m}$ ]] |
| $q_i$                     | Modal coordinate [m]                           | $\vartheta_i$       | Critical damping [-]                        |
| $\dot{q}_i$               | Modal velocity [m/s]                           | $\omega_{0,i}$      | Eigenfrequency [1/s]                        |
| $\ddot{q}_i$              | Modal acceleration [m/s <sup>2</sup> ]         | $\Omega$            | Excitation frequency [1/s]                  |
| $\hat{q}_i$               | Modal amplitude [m]                            | $\Omega_{res}$      | Excitation frequency at resonance [1/s]     |

## References

- [1] Marinkovic, D., Zehn, M., Survey of finite element method-based real-time simulations, *Applied Sciences*, 9(14), 2019, 2775.
- [2] Marinkovic, D., Zehn, M., Pavlovic, A., Highly efficient FE simulations by means of simplified corotational formulation, *Operational Research in Engineering Sciences: Theory and Applications*, 3(2), 2020, 74-86.
- [3] Mastrogiannakis, I., Vosniakos, G.-C., Exploring structural design of the Francis hydro-turbine blades using composite materials, *Facta Universitatis-Series Mechanical Engineering*, 18(1), 2020, 43-55.
- [4] Ahmadifar, A., Zamani, M.R., Davar, A., Jam, J.E., Beni, M. H., Experimental and numerical buckling analysis of carbon fiber composite lattice conical structure before and after lateral impact, *Journal of Applied and Computational Mechanics*, 6(4), 2020, 813-822.
- [5] Fallahi, N., Viglietti, A., Carrera, E., Pagani, A., Zappino, E., Effect of fiber orientation path on the buckling, free vibration and static analyses of variable angle tow panels, *Facta Universitatis-Series Mechanical Engineering*, 18(2), 2020, 165-188.
- [6] Rama, G., Marinkovic, D., Zehn, M., High performance 3-node shell element for linear and geometrically nonlinear analysis of composite laminates, *Composites Part B: Engineering*, 151, 2018, 118-126.
- [7] Marinković, D., Rama, G., Zehn, M., Abaqus implementation of a corotational piezoelectric 3-node shell element with drilling degree of freedom, *Facta Universitatis-Series Mechanical Engineering*, 17(2), 2019, 269-283.
- [8] Rama, G., Marinković, D., Zehn, M., Efficient three-node finite shell element for linear and geometrically nonlinear analyses of piezoelectric laminated structures, *Journal of Intelligent Material Systems and Structures*, 29(3), 2018, 345-357.
- [9] Pavlovic, A., Fragassa, C., Geometry optimization by FEM simulation of the automatic changing gear, *Reports in Mechanical Engineering*, 1(1), 2020, 199-205.
- [10] Ye, Y., Zhu, W., Jiang, J., Xu, Q., Ke, Y., Design and optimization of composite sub-stiffened panels, *Composite Structures*, 240, 2020, 112084.
- [11] Miao, B.R., Luo, Y.X., Peng, Q.M., Qiu, Y.Z., Chen, H., Yang, Z.K., Multidisciplinary design optimization of lightweight carbody for fatigue assessment, *Materials & Design*, 194, 2020, 108910.
- [12] Minak, G., Brugo, T., Fragassa, C., Pavlovic, A., Zavatta, N., De Camargo, V. F., Structural Design and Manufacturing of a Cruiser Class Solar Vehicle, *Journal of Visualized Experiments*, 143, 2019, e58525.
- [13] Paz, M., *Structural dynamics: theory and computation*, Springer Science & Business Media, 2012.
- [14] Marinković, D., Zehn, M., Consideration of stress stiffening and material reorientation in modal space based finite element solutions, *Physical Mesomechanics*, 21(4), 2018, 341-350.
- [15] Pavlovic, A., Sintoni, D., Minak, G., Fragassa, C., On the Modal Behaviour of Ultralight Composite Sandwich Automotive Panels, *Composite Structures*, 248, 2020, 112523.
- [16] Fragassa, C., Pavlovic, A., Minak, G., On the Structural Behaviour of a CFRP Safety Cage in a Solar Powered Electric Vehicle, *Composite Structures*, 252, 2020, 112698.
- [17] Pavlovic, A., Fragassa, C., Investigating the resistance of concrete reinforced walls to high velocity projectiles, *Engineering Structures*, 174, 2018, 384-395.
- [18] Craig, R., Kurdila, A., *Fundamentals of Structural Dynamics. 2nd ed.*, John Wiley & Sons, New Jersey, 2006.
- [19] Huang, L., Agrawal, H., Kurudiyara, P., Dynamic Durability Analysis of Automotive Structures, *SAE Transactions*, 1998, 474-480.
- [20] Brincker, R., Ventura, C., *Introduction to Operational Modal Analysis*, John Wiley & Sons, Chichester, 2015.
- [21] Lopez-Aenlle, M., Brincker, R., Fernandez, P., Fernandez-Canteli, A., On exact and approximated formulations for scaling mode shapes in operational modal analysis by mass and stiffness change, *Journal of Sound and Vibration*, 331(3), 2012, 622-637.
- [22] Bernal, D., A receptance based formulation for modal scaling using mass perturbations, *Mechanical Systems and Signal Processing*, 25(2), 2011, 621-629.
- [23] Brownjohn, J.M.W., Pavic, A., Experimental methods for estimating modal mass in footbridges using human-induced dynamic excitation, *Engineering Structures*, 29(11), 2007, 2833-2843.
- [24] Yam, L.Y., Leung, T.P., Li, D.B., Xue, K.Z., Theoretical and experimental study of modal strain analysis, *Journal of Sound and Vibration*, 191(2), 1996, 251-260.
- [25] Lu, G.Y., Zheng, D., Venkatakrishnaiah, S., Vest, T., A Dynamic Durability Analysis Method and Application to a Battery Support Subsystem, *SAE Technical Paper*, 2004, No. 2004-01-0874.
- [26] Vellaichamy, S., Keshtkar, H., New approaches to modal transient fatigue analysis, *SAE Transactions*, 2000, 845-850.
- [27] Mršnik, M., Slavič, J., Boltežar, M., Vibration fatigue using modal decomposition, *Mechanical Systems and Signal Processing*, 98, 2018, 548-556.
- [28] Braccisi, C., Cianetti, F., Tomassini, L., An innovative modal approach for frequency domain stress recovery and fatigue damage evaluation, *International Journal of Fatigue*, 91, 2016, 382-396.
- [29] Lu, Y., Xiang, P., Dong, P., Zhang, X., Zeng, J., Analysis of the effects of vibration modes on fatigue damage in high-speed train bogie frames, *Engineering Failure Analysis*, 89, 2018, 222-241.
- [30] Albuquerque, C., Silva, A.L., de Jesus, A.M., Calçada, R., An efficient methodology for fatigue damage assessment of bridge details using modal



superposition of stress intensity factors, *International Journal of Fatigue*, 81, 2015, 61-77.

- [31] Gu, Z., Mi, C., Wang, Y., Jiang, J., A-type frame fatigue life estimation of a mining dump truck based on modal stress recovery method, *Engineering Failure Analysis*, 26, 2012, 89-99.
- [32] Horas, C.S., Correia, J.A.F.O., De Jesus, A.M.P., Calçada, R., Aenlle, M.L., Kripakaran, P., Fernandez-Canteli, A., Application of modal superposition technique in the fatigue analysis using local approaches, *Procedia Engineering*, 160, 2016, 45-5.
- [33] Tran, V.X., Geniaut, S., Galenne, E., Nistor, I., A modal analysis for computation of stress intensity factors under dynamic loading conditions at low frequency using extended finite element method, *Engineering Fracture Mechanics*, 98, 2013, 122-136.
- [34] Huang, L., Agrawal, H., Borowski, V., Durability analysis of a vehicle body structure using modal transient methods, *Proceedings of the 15th International Modal Analysis Conference*, Orlando, Florida, 407-414, 1997.
- [35] Lesiuk, G., Smolnicki, M., Mech, R., Ziety, A., Fragassa, C., Analysis of fatigue crack growth under mixed mode (I + II) loading conditions in rail steel using CTS specimen, *Engineering Failure Analysis*, 109, 2020, 104354.
- [36] Huang, L., Agrawal, H., US Patent No. 6212486, 2001.
- [37] Lin, R.M., Mottershead, J.E., Ng, T.Y., A state-of-the-art review on theory and engineering applications of eigenvalue and eigenvector derivatives, *Mechanical Systems and Signal Processing*, 138, 2020, 106536.
- [38] Tigh Kuchak, A.J., Marinkovic, D., Zehn, M., Finite element model updating - Case study of a rail damper, *Structural Engineering and Mechanics*, 73(1), 2020, 27-35.
- [39] Fotouhi, S., Akrami, R., Ferreira-Green, K., Naser, G., Fotouhi, M., Fragassa, C., Piezoelectric PVDF sensor as a reliable device for strain/load monitoring of engineering structures, *IOP Conference Series: Materials Science and Engineering*, 659(1), 2019, 012085.
- [40] Fragassa, C., Minak, G., Pavlovic, A. Measuring Deformations in a Telescopic Boom under Static and Dynamic Load Conditions, *Facta Universitatis-Series Mechanical Engineering*, 18(2), 2020, 315-328.
- [41] Pavlovic, A., Sintoni, D., Fragassa, C., Minak, G., Multi-Objective Design Optimization of the Reinforced Composite Roof in a Solar Vehicle, *Applied Sciences*, 10, 2020, 2665.
- [42] Veltri, M., FEM Techniques for High Stress Detection in Accelerated Fatigue Simulation, *Journal of Physics: Conference Series*, 744, 2016, 012137.
- [43] Zhou, Y., Wu, S., Trisovic, N., Fei, Q., Tan, Z., Modal Strain Based Method for Dynamic Design of Plate-Like Structures, *Shock and Vibration*, 2016, 2016, 2050627.
- [44] Zhou, Y., Fei, Q., Wu, S., Utilization of modal stress approach in random-vibration fatigue evaluation, *Proceedings of the Institution of Mechanical Engineers, Part G: Journal of Aerospace Engineering*, 231(14), 2017, 2603-2615.
- [45] Zhou, Y., Tao, J., Theoretical and numerical investigation of stress mode shapes in multi-axial random fatigue, *Mechanical Systems and Signal Processing*, 127, 2019, 499-512.
- [46] Strzalka, C., Zehn, M., The influence of loading position in a priori high stress detection using mode superposition, *Reports in Mechanical Engineering*, 1(1), 2020, 93-102.
- [47] Clough, R.W., Penzien, J., *Dynamics of Structures*, McGraw-Hill, New York, 1975.
- [48] Aenlle, M., Juul, M., Brincker, R., Modal Mass and Length of Mode Shapes in Structural Dynamics, *Shock and Vibration*, 2020, 2020, 8648769.

## ORCID iD

Carsten Strzalka  <https://orcid.org/0000-0002-8490-5899>

Dragan Marinkovic  <https://orcid.org/0000-0002-3583-9434>

Manfred W. Zehn  <https://orcid.org/0000-0002-2412-3676>



© 2021 Shahid Chamran University of Ahvaz, Ahvaz, Iran. This article is an open access article distributed under the terms and conditions of the Creative Commons Attribution-NonCommercial 4.0 International (CC BY-NC 4.0 license) (<http://creativecommons.org/licenses/by-nc/4.0/>).

**How to cite this article:** Strzalka C., Marinkovic D., Zehn M.W. Stress Mode Superposition for a Priori Detection of Highly Stressed Areas: Mode Normalisation and Loading Influence, *J. Appl. Comput. Mech.*, 7(3), 2021, 1698-1709. <https://doi.org/10.22055/JACM.2021.36637.2878>

**Publisher's Note** Shahid Chamran University of Ahvaz remains neutral with regard to jurisdictional claims in published maps and institutional affiliations.

